11-2012

"Tuning hole mobility in InP nanowires"

Mariama Rebello Sousa Dias
University of Richmond, mdias@richmond.edu

A. Picinin

V. Lopez-Richard

S. E. Ulloa

L. K. Castelano

See next page for additional authors

Recommended Citation

Rebello Sousa Dias, M., A. Picinin, V. Lopez-Richard, S.E. Ulloa, L.K. Castelano, J.P. Rino, G.E. Marques. "Tuning hole mobility in InP nanowires," *Applied Physics Letters* 101,182104 (2012). https://doi.org/10.1063/1.4764902.

Authors
Mariama Rebello Sousa Dias, A. Picinin, V. Lopez-Richard, S. E. Ulloa, L. K. Castelano, J. P. Rino, and G. E. Marques

Tuning hole mobility in InP nanowires

M. Rebello Sousa Dias,[1,2] A. Picinin,[1] V. Lopez-Richard,[1] S. E. Ulloa,[2] L. K. Castelano,[1] J. P. Rino,[1] and G. E. Marques[1]
[1]*Departamento de Física, Universidade Federal de São Carlos, 13565 905 São Carlos, São Paulo, Brazil*
[2]*Department of Physics and Astronomy and Nanoscale and Quantum Phenomena Institute, Ohio University, Athens, Ohio 45701 2979, USA*

(Received 10 April 2012; accepted 16 October 2012; published online 1 November 2012)

Transport properties of holes in InP nanowires (NWs) were calculated considering electron-phonon interaction via deformation potentials, the effect of temperature, and strain fields. Using molecular dynamics, we simulate NW structures, the longitudinal optical phonon (LO-phonon) energy renormalization, and lifetime. The valence band ground state changes between light- and heavy-hole character, as the strain fields and the NW size vary. Drastic changes in the mobility arise with the onset of resonance between the LO-phonons and the separation between valence subbands.

Semiconductor nanowires (NWs) are increasingly used in a wide range of devices. They appear as building blocks of nanocircuits[1] and can be applied in electrically driven lasing,[2] which can be used in telecommunications and information storage for medical diagnostics and therapeutics.[3] Improvements in NW synthesis, including chemical techniques, allow thorough control of their shape, size, and composition[4–6] along with detailed microscopic characterization of built-in strain fields.[6,7] As the conductivity is mostly defined by the carrier-phonon interaction and phonon-lifetime, tuning of the NW structural properties could result in the possibility of also finding optimal conditions for carrier transport. Considerable efforts have been devoted to the description of carriers in the conduction band of NWs,[8–10] while similar endeavors are not so common for holes in the valence band.[11] As the mobility is inversely proportional to the carrier effective mass, one may naturally expect that considering carriers in the valence band may result in a drop in mobility when compared to the light electrons in the conduction band. This could certainly be the case for heavy-hole (hh) transport; however, light-holes (lh) under certain conditions may be promoted to be the top valence band by tuning NWs structural parameters.[12] Such characteristics are directly linked to technological problems as for instance the reduction of losses in interconnection in nanocircuits, enhancement of photocells efficiency by boosting the charge collection,[13] and controllability of the carrier thermal conductivity.[14]

In this work, we considered InP NWs parameters given the relevance of this material in proposals for NW photodetectors[15] and nano-circuit applications,[16,17] although the obtained results can be generalized to other zinc-blende NWs. To probe the possible changes in the hole character, we consider effects due to confinement, hh-lh mixing, and strain and surface asymmetry fields.[6,12] As shown in this work, these effects lead to a significant mobility enhancement for lh in suitable NWs. We can also take advantage of valence band mass anisotropy to attain resonant conditions that allow sharp variations of the hole mobility with external parameters, especially when the leading scattering process involves longitudinal optical phonons (LO-phonons) through the deformation potential.[18] Additional hole-phonon interactions,[19] such as deformation potential and piezoelectric coupling to acoustic phonons and polar coupling to optical phonons,[20] have weaker effects and will not be considered here.[19,21] In order to provide realistic estimates of the expected mobility changes in the NWs of interest, we consider the effects of dimensionality reduction on the LO-phonon dispersion and lifetime, using molecular dynamics (MD) simulations for different NWs sizes and at various temperatures. We consider different NW cross sections and shapes, while temperature effects are included in the mobility through the phonon occupation and strain effects in a multiband Luttinger Hamiltonian. We find that mobility changes drastically according to NW width, strain fields, and temperature. In particular, we show that for certain NW widths, one finds resonant behaviors that greatly suppress the hole mobility and are strongly affected by temperature and strain.

The interaction potentials used in our MD simulations consist of two- and three-body interaction terms, as described by Branicio *et al.*[22,23] The parameters of the interatomic potential are determined using the cohesive energy, density, bulk modulus, and elastic constant C_{11} of the material as described before.[23] This potential provides excellent estimates for the vibrational density of states, melting temperature, structural phase transformation induced by pressure, and specific heat.[22] The NWs were created cutting a block of a perfect crystal with the z-axis along the [001] direction with periodic boundary conditions in the z-direction. The x- and y-directions were surrounded by a vacuum region. The system is typically composed of nine unit cells along x- and y-directions and forty unit cells along the z-direction (53 Å × 53 Å × 234.5 Å); the total number of atoms is 25 920 (12 960 In + 12 960 P) (inset Fig. 1). The NW is allowed to relax during a long simulation run (25 000 time steps, one time step = 1.5 fs) at each temperature. After this relaxation process, a few surface defects can be observed in inset Fig. 1.

Given the velocity-velocity auto correlation function, $Z(t) = \frac{\langle \vec{v}_i(t).\vec{v}_i(0)\rangle}{\langle \vec{v}_i(0).\vec{v}_i(0)\rangle}$, where $\vec{v}_i(t)$ is the velocity of particle i at time t and the brackets are averages over ensembles and

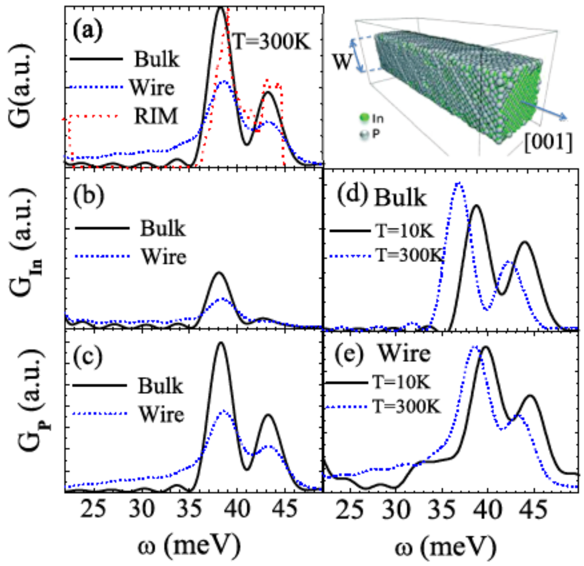

FIG. 1. VDOS for NW and bulk. (a) Total VDOS; RIM VDOS for bulk from data.[26] (b) and (c) Partial VDOS for bulk and NW at 300 K: (b) indium contribution and (c) phosphorus contribution. (d) and (e) VDOS for bulk and NW at 10 K and 300 K. Inset: Simulated InP NW structure by molecular dy namics at T 300 K. Green (grey) dots represent indium (phosphorous) atoms.

particles, we determine the vibrational phonon density of states (VDOS) through the Fourier transform[24]

$$G_l(\omega) = \frac{6N_l}{\pi}\int_0^{\infty} Z_l(t)\cos(\omega t)dt, \tag{1}$$

where the subindex l is related to the atom In or P.

Fig. 1(a) compares the VDOS computed from MD calculations for a bulk system (solid curve) to the VDOS extracted from the rigid ion model (RIM) (dashed curve), which is based on experimental results.[25,26] The MD results reproduce very well the main characteristics of the experimental results, predicting the existence of the transversal optical (TO, ∼43 meV) and LO (∼38 meV) modes, and a gap between 22 meV and 36 meV (acoustic modes below 22 meV not shown). The effect of the surfaces on the VDOS of the NW is also shown in Figs. 1(a) 1(c). The main NW characteristics in the VDOS resemble the bulk results; however, some differences can be observed. The presence of the NW surface increases the density of modes in the gap region, between 22 meV and 36 meV, although the TO and LO modes remain dominant. To extract more information about the origin of the modes, we show in Figs. 1(b) and 1(c) the partial VDOS for bulk and InP NW considering the In and P contribution separately. We notice that the P atoms make the main contribution to the optical modes, because such modes are characterized by the relative displacement between ions and lighter atoms usually dominate such dynamics. Furthermore, we observe for the NW a slight blue shift of the LO mode (∼1 meV) with respect to the bulk.

The effect of temperature on the VDOS for both NW and bulk structure is shown in Figs. 1(d) and 1(e). We see a general broadening of the modes and a shift in the peak position to lower frequencies when the temperature is raised. Although the gap region keeps a similar profile, the VDOS increases with temperature. Moreover, the temperature affects the contrast between LO and TO modes, especially for the NW, where the LO frequency width increases as shown in Fig. 1(e). Notice that the mode broadening is slightly weaker for the NW than for the bulk. Also, the NW exhibits a shift in the LO mode with temperature, which is an important fact to be considered when calculating the contribution of hole-phonon scattering to the mobility.

To describe the valence band for NWs taking into account confinement effects, mass anisotropy, and strain fields within the same framework, we employ the Luttinger Hamiltonian,[27]

$$\mathcal{H}_{hh(lh)} = -\left(\frac{\gamma_1 \pm \gamma_2}{2}\right)\{\hat{k}_+, \hat{k}\ \ \} - \left(\frac{\gamma_1 \mp 2\gamma_2}{2}\right)\hat{k}_z^2, \tag{2}$$

for the hh and lh, where γ_α $(\alpha = 1, 2, 3)$ are the Luttinger parameters, $\{A, B\} = \frac{1}{2}(AB + BA)$, and $\hat{k}_\pm = \hat{k}_x \pm i\hat{k}_y$. The subband with hh character along the wire has a *low* effective mass in the transverse direction $\sim(\gamma_1 + \gamma_2)^{\ 1}$, while the lh subband has a *large* transverse mass $\sim(\gamma_1 - \gamma_2)^{\ 1}$; the different transverse masses result in the possible inversion of the lh and hh subband ordering, due to the NW confinement effects. Strain fields lead to modulation of the valence subbands[6] by inducing a subband displacement given by[28] $\Delta\mathcal{H}_{hh} = -P + Q$ and $\Delta\mathcal{H}_{lh} = -P + Q + \frac{2Q^2}{\Delta_{so}}$, where $P = 2(a_v + a_c)(\frac{c_{11}+c_{12}}{c_{11}})\varepsilon_{||}$, $Q = -b(\frac{c_{11}+2c_{12}}{c_{11}})\varepsilon_{||}$ and $\Delta_{so} = 0.108$ eV is the spin-orbit split-off energy.[6,29,30]

The hole wave function in the NW has the form $|\Psi_i\rangle = |\psi_i\rangle|J, m_j\rangle$, where $|\psi_i\rangle$ is the envelope function, which depends on the cross section of the NW, and $|J, m_j\rangle$ is the total angular momentum eigenstate, $|3/2, \pm 3/2\rangle$ for pure hh character, and $|3/2, \pm 1/2\rangle$ for the lh.

The hole-phonon interaction Hamiltonian is given by

$$\mathcal{H}_{h\ \ p} = \sum_{\mathbf{q}} M_{\mathbf{q}} U_{h\ \ i}(\mathbf{q})[\hat{a}_{\mathbf{q}} e^{i\mathbf{r}\cdot\mathbf{q}} + \hat{a}_{\mathbf{q}}^{\dagger} e^{\ \ i\mathbf{r}\cdot\mathbf{q}}], \tag{3}$$

with $M_{\mathbf{q}} = (\mathbf{q}\cdot\varepsilon_q)(\hbar/2\rho\omega_{\mathbf{q}}V)^{\frac{1}{2}}$, where $\mathbf{q}$ is the phonon wave vector for polarization vector ε_q, ρ is the mass density, V is the system volume, and $U_{h\ \ i}(\mathbf{q})$ is given in terms of the deformation potential for holes.[21] Considering long wavelength processes, we have $U_{h\ \ i}(\mathbf{q}) \propto \mathbf{u}$, where $\mathbf{u}$ is the relative displacement between atoms inside the primitive unit cell. By symmetry, states with hh character couple with those of lh character along the direction [001].[21] Because this direction coincides with the wire axis, along which the carrier transport takes place, we find $\langle hh^{\pm}|U_{h\ \ i}(z)|lh^{\mp}\rangle = \langle lh^{\mp}|U_{h\ \ i}(z)|hh^{\pm}\rangle = \frac{\pm i d_0}{2a_0}$, where d_0 is the deformation constant and a_0 the lattice parameter.[31]

The mobility is given by $\mu = \frac{e}{m_0\lambda_{z\beta}}\tau$, where $\tau^{\ 1} = \sum_q S(k, q)$ is the hole-phonon scattering time and the transition rate can be calculated as follows

$$S(k, k') = \frac{2\pi}{\hbar}[|\langle\mathcal{H}^a_{h\ \ p}\rangle|^2\delta(E_f(k') - E_i(k) - \hbar\omega_{\mathbf{q}}) + |\langle\mathcal{H}^e_{h\ \ p}\rangle|^2\delta(E_f(k') - E_i(k) + \hbar\omega_{\mathbf{q}})], \tag{4}$$

where k and k' refer to the initial and final states, and $\mathcal{H}^a_{h\ \ p}$ and $\mathcal{H}^e_{h\ \ p}$ refer to the phonon absorption and emission processes in Eq. (3). The phonon density is assumed to be given by a Lorentzian centered at ω_{LO} and with width γ. Both of these values shift with temperature, as demonstrated by the MD simulation.

To characterize the initial and final states involved in the scattering processes that affect the mobility, we schematically show in Fig. 2 the relevant valence band structure for two different cases. For thin NWs, with or without strain, the finite NW width leads to a picture similar to Fig. 2(a), where the lh subband is promoted to the top due to its higher transverse effective mass. Thus, under such conditions, a hh can be scattered to the subband with lh character through phonon emission (process E_1), and at $T > 0$ the lh can be excited to the hh subband via phonon absorption (process A_1). In the presence of lateral compressive strain, the subbands may switch their relative positions and the hh assumes the top for thicker NWs. In such a situation, a lh might be scattered via phonon emission (process E_2) while a hh can be affected by phonon absorption at $T > 0$ (process A_2). Notice that by changing the wire radius, one can reach a resonant condition ($\Delta E_{vb} = \hbar\omega_{LO}$).

The relative position of the valence subbands is extremely important for the carrier transport in NWs because the mobility dependence on the longitudinal effective mass. In particular, temperature or structural parameters may drastically affect the valence subbands, thereby inducing sharp fluctuations on the mobility. To probe such effects, in Fig. 3 we plot the mobility for different strain and temperature values as a function of the NW width.

Fig. 3(a) shows that the mobility is enhanced after a certain NW width, where ΔE_{vb} becomes smaller than $\hbar\omega_{LO}$, consequently inhibiting the condition for resonant phonon emission for the hh. While the subbands approach (by increasing the NW width), the lh mobility monotonically decreases due to increased phonon emission probability. Therefore, the sharp variation observed in panel (a) corresponds to the condition where the LO-phonon emission by a hh is switched-off by increasing the NW width. At higher temperatures, Fig. 3(b), a resonant transition by phonon absorption also affects the carriers in the lh subband, producing a sharp drop in mobility (due to A_1 processes shown in Fig. 2(a)) when the corresponding inter-subband transitions are switched-on.

Given the band structure modulation with strain, the condition $|\Delta E_{vb}| \sim \hbar\omega_{LO}$ can be attained twice by varying the NW width (corresponding to the cases displayed in Figs. 2(a) and 2(b)). Thus, two resonant regions appear in Fig. 3(c), where phonons can be emitted by both hh and lh subbands (E_1 an E_2 processes, respectively). At higher temperatures, the phonon absorption features appear as additional jumps in the mobility due to processes A_1 and A_2 as depicted in Fig. 3(d). Analogously to the unstrained case, by increasing the NW width one can attain conditions when the resonant transitions are switched-off (on) for the hh (lh). Tuning the mobility of a hole system via *in-situ* changes of the NW width or strain fields is not an easy task in experiments. However, one can achieve drastic *in-situ* mobility changes for NWs close to the resonance condition by suitable changes in temperature. Note that, any time a phonon emission or absorption process is allowed, the mobility is reduced from the uncoupled case; however, Fig. 3 compares the mobility enhancement or reduction with NW width.

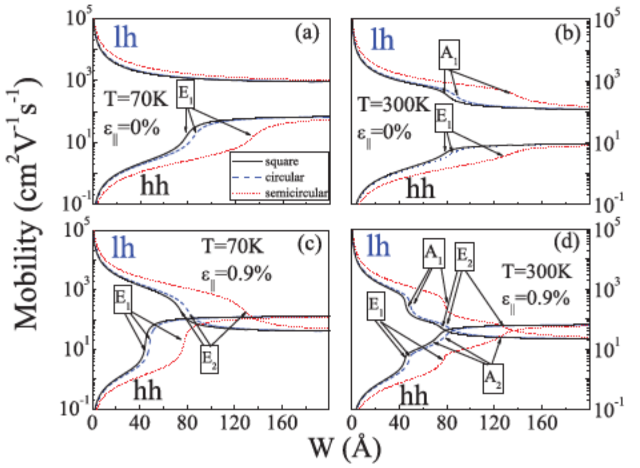

FIG. 3. Hole mobility versus NW width W for states with k_z 0. (a) System at T 70 K without strain. (b) System at T 300 K without strain. (c) System at T 70 K with strain. (d) System at T 300 K with strain.

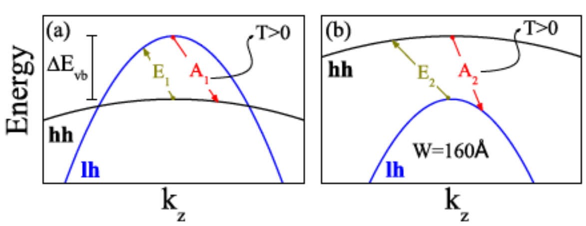

FIG. 2. Valence band ground states for NW of width W. (a) When the lh occupies the ground state. (b) When the hh occupies the ground state.

In Fig. 4(a), we consider a square NW with width $W = 20$ Å; no resonant signatures appear in the strain and temperature range analyzed because $\Delta E_{vb} > \hbar\omega_{LO}$. On the other hand, such conditions become evident for both kinds of holes when thicker NWs ($W = 50$ Å) are considered. In addition, by raising the temperature, the process of phonon

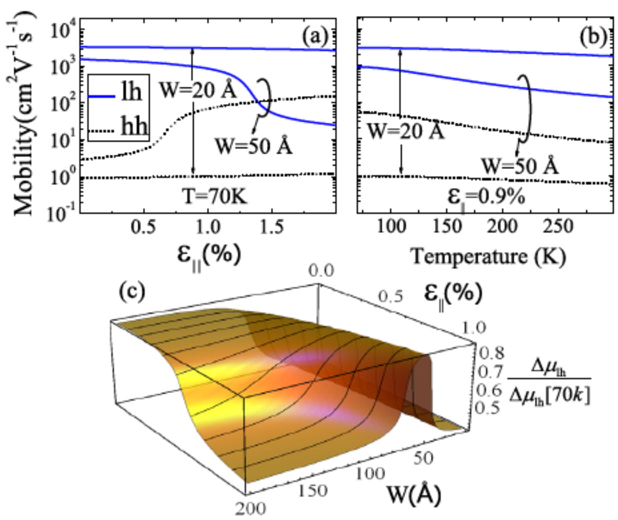

FIG. 4. (a) and (b) Hole mobility for two values of NW width for states with k_z 0: (a) as function of strain for T 70 K, and (b) as function of temperature for $\varepsilon_{||}$ 0.9%. (c) Relative light hole mobility fluctuation, where $\Delta\mu_{lh}$ (μ_{lh}[70 K] μ_{lh}[300 K]), versus wire width for different values of strain at k_z 0.

absorption becomes more effective and the lh mobility is reduced, as displayed in Fig. 4(b). Such effect is present for NWs with different widths and strains.

Fig. 4(c) shows the relative lh mobility fluctuation, $\Delta\mu_{lh}/\mu_{lh}[70\,\mathrm{K}]$, where $\Delta\mu_{lh} = (\mu_{lh}[70\,\mathrm{K}] - \mu_{lh}[300\,\mathrm{K}])$, as a function of the NW width for different values of strain. For lh, the mobility at low temperatures is high (Fig. 4(b)). Moreover, one may observe a drastic drop in mobility at high temperature depending on the NW width and strain. For a system without strain, a large but monotonic drop in the mobility is achieved for NWs with width larger than 100 Å. In real systems, however, free standing NWs grow with built-in strain,[6] which has a direct impact on the dependence of μ on temperature and width. As the strain increases, the lh-hh subband reversal is possible depending on the NW width, thereby resulting in a highly sensitive mobility on temperature and/or width. For example, for $\varepsilon_{||} = 0.9\%$,[6] and for width values close to 50 Å, the mobility exhibits a sharp change as a function of the temperature.

In summary, the hole mobility in InP semiconductor NWs can be tuned by the NW size, strain field modulation, and temperature conditions. The MD with realistic force potentials allowed the characterization of the LO-phonon energy renormalization due to the reduced dimensionality and variations of the phonon lifetimes with temperature. These features are essential ingredients for the characterization of carrier mobility. The fact that the ground state can switch character between hh and lh with strain and/or size is also highlighted. In addition, steep variation of the mobility can be attained when the energy separation between the two valence subbands equals the LO-phonon energy. These conditions can be tuned by size or strain fields and are also affected by temperature, and should be taken into careful consideration when designing possible NW-based devices. The extension of these results to other III-V NWs with zinc-blende structure is straightforward, leading to analogous qualitative behavior. Yet, for instance, InAs NWs would present higher lh-mobility due to the relatively lower mass ($m_{lh} \sim 0.027$) if compared to InP ($m_{lh} \sim 0.12$) NWs.

The authors acknowledge the support of CAPES, CNPQ, and FAPESP (Brazil), and NSF MWM/CIAM (US).

[1] H. A. Nilsson, C. Thelander, L. E. Froberg, J. B. Wagner, and L. Samuelson, Appl. Phys. Lett. **89**, 163101 (2006).
[2] X. Duan, Y. Huanh, R. Agarwal, and C. M. Lieber, Nature **421**, 241 245 (2003).
[3] G. R. Gray, *Semiconductor Laser: Past, Present, and Future* (American Intitute of Physics, New York, 1995).
[4] M. S. Gudiksen and C. M. Lieber, J. Am. Chem. Soc. **122**, 8801 8802 (2000).
[5] M. T. Bjork, B. J. Ohlsson, A. I. Persson, C. Thelander, M. H. Magnusson, K. Deppert, L. R. Wallenberg, and L. Samuelson, Nano Lett. **2**, 87 (2002).
[6] V. Lopez Richard, J. C. Gonzalez, F. M. Matinaga, C. Trallero Giner, E. Ribeiro, M. Rebello Sousa Dias, L. Villegas Lelovsky, and G. E. Marques, Nano Lett. **9**, 3129 (2009).
[7] L. Villegas Lelovsky, C. Trallero Giner, M. Rebello Sousa Dias, V. Lopez Richard, and G. E. Marques, Phys. Rev. B **79**, 155306 (2009).
[8] D. Huang and G. Gumbs, J. Appl. Phys. **107**, 103710 (2010).
[9] T. Fang, A. Konar, H. Xing, and D. Jena, Phys. Rev. B **78**, 205403 (2008).
[10] M. Tsetseri and G. P. Triberis, Phys. Rev. B **69**, 075313 (2004).
[11] F. Murphy Armando, G. Fagas, and J. C. Greer, Nano Lett. **10**, 869 873 (2010).
[12] M. Rebello Sousa Dias, "Estudo de efeitos qunticos nas propriedades eletrnicas de nanofios semicondutores," Master's thesis (Departamento de Física, Universidade Federal de Sao Carlos, 2010).
[13] A. I. Hochbaum and P. Yang, Chem. Rev. **110**, 527 546 (2010).
[14] A. M. Katzenmeyer, F. Leonard, A. A. Talin, M. E. Toimil Molares, J. G. Cederberg, J. Y. Huang, and J. L. Lensch Falk, IEEE Trans. Nanotechnol. **10**, 92 (2011).
[15] H. Pettersson, I. Zubritskaya, N. T. Nghia, J. Wallentin, M. T. Borgstrom, K. Storm, L. Landin, P. Wickert, F. Capasso, and L. Samuelson, Nanotech nology **23**, 135201 (2012).
[16] M. Heurlin, P. Wickert, S. Falt, M. T. Borgstrom, K. Deppert, L. Samuel son, and M. H. Magnusson, Nano Lett. **11**, 2028 (2011).
[17] C. J. Novotny, E. T. Yu, and P. K. L. Yu, Nano Lett. **8**, 775 (2008).
[18] V. Lopez, G. E. Marques, J. Drake, and C. Trallero Giner, Phys. Rev. B **56**, 15691 (1997).
[19] G. G. Mahan, *Many Particle Physics*, 3rd ed. (Kluwer, New York, 2000).
[20] V. Lopez Richard, G. E. Marques, C. Trallero Giner, and J. Drake, Phys. Rev. B **58**, 16136 (1998).
[21] P. Y. Yu and M. Cardona, *Fundamentals of Semiconductors* (Springer, Berlin, 1996).
[22] P. S. Branicio, J. P. Rino, G. C. Kwan, and H. Tsuzuk, J. Phys.: Cond. Matter **21**, 095002 (2009).
[23] H. Tsuzuki, C. D. Ferreira, M. Rebello Sousa Dias, L. K. Castelano, V. Lopez Richard, J. P. Rino, and G. E. Marques, ACS Nano **5**, 5519 (2011).
[24] J. P. Rino, Y. M. M. Hornos, G. A. Antonio, I. Ebbsjo, R. K. Kalia, and P. Vashishta, J. Chem. Phys. **89**, 7542 (1988).
[25] P. H. Borcherds, G. F. Alfrey, A. D. B. Woods, and D. H. Saunderson, J. Phys. C **8**, 2022 2030 (1975).
[26] H. Bilz and W. Kress, *Phonon Dispersion Relations in Insulators*, Springer Series in Solid State Sciences Vol. 10 (Springer Verlag, 1979).
[27] J. M. Luttinger, Phys. Rev. **102**, 1030 (1956).
[28] F. H. Pollak and M. Cardona, Phys. Rev. **172**, 816 (1968).
[29] *Landolt Bornstein Comprehensive Index*, edited by O. Madelung and W. Martienssen (Springer, Berlin, 1996).
[30] D. D. Nolte, W. Walukiewicz, and E. E. Haller, Phys. Rev. Lett. **59**, 501 (1987).
[31] A. Cantarero, C. Trallero Ginger, and M. Cardona, Phys. Rev. B **39**, 8388 (1989).